The development of analytical methods for the purity determination of fucoidan extracted from brown seaweed species

Ming Zhao [1], Marco Garcia-Vaquero [2], Joanna Przyborska [3], Saravana Periaswamy Sivagnanam [1], Brijesh Tiwari [1]

[1] Department of Food Chemistry and Technology, Teagasc Food Research Centre, Ashtown, Dublin 15, Ireland

[2] School of Agriculture and Food Science, University College Dublin, Belfield, Dublin 4, Ireland

[3] Shannon Applied Biotechnology Centre, Institute of Technology Tralee, Tralee, Co. Kerry, Ireland

Abstract

To determine the purity of extracted fucoidan from brown seaweeds, analytical methods were developed, including spectroscopy (i.e., Attenuate total reflectance (ATR) - Fourier-transform infrared (FT-IR) and Raman) combined with chemometrics; and the results were compared with those of high performance liquid chromatography (HPLC) and other two chemistry methods (i.e. fucoidan estimation based on fucose content and a cationic dye method based on sulphated polysaccharide estimation). Quantitative models (i.e., partial least squares regression (PLSR)) were developed and cross-validated using FT-IR spectroscopic methods (R2CV ~ 0.998, RMSECV ~1.7%). The models were also validated using other four commercial fucoidan products. On the other hand, the same commercial samples were used to validate the two chemistry methods and the HPLC method. Estimation results of these analytical methods were discussed based on the potential of these analytical methods for fucoidan purity determination. The results demonstrated FT-IR spectroscopy with chemometrics potentially could be used for non-destructive and real time determination.

Highlights

- Purity determination of fucoidan extracted from brown seaweeds were investigated.
- FT-IR and Raman with chemometrics were employed to develop the analytical methods.
- HPLC and two chemistry methods were also used for fucoidan purity estimation.
- The pros and cons of all the analytical methods were discussed.

Keywords

Fucoidan contentAttenuate total reflectance - Fourier-transform infrared (ATR-FT-IR)RamanChemometricsAnalytical methodsHigh performance liquid chromatography (HPLC)

1. Introduction

Fucoidan is a sulphated polysaccharide containing L-fucose in the linear or branched structures and other monosaccharides, i.e., D-galactose, D-mannose, D-xylose, d-glucose and uronic acids, etc. [1,2]. The basic chemical structure of fucoidan consists of a polymer of α-(1 → 2), α-(1 → 3) or α-(1 → 4) linked L-fucose with sulphate groups attached at the C2 or/and C3, C4 position on some L-fucopyranose residues; fucose branches was also attached to the polymer chain on every two or three fucose residues [[3], [4], [5]]. Fucoidan has been found in some marine invertebrates (e.g., sea urchins and sea cucumbers) and in the cell wall of brown seaweed species (e.g., Fucales, Laminariales, Chordariales and Ectocapales) [[6], [7], [8], [9]].

Since centuries ago, fucoidan has been consumed as dietary fiber in Asian countries; whereas, in recent years, the bio-activities of fucoidan have been proven for the effects of anti-inflammatory, anti-virus, anti-tumor, anticoagulant, antioxidant and other immunomodulatory activities to against neuropathy, gastropathy, hepatopathy, uropathy and renalpathy [5,10,11]. As another reason that brown seaweeds have been naturally cultivated in a large scale and distributed along the coastline of many countries, fucoidan isolation from brown seaweeds has gained increasing attention in the pharmaceutical and functional food industries [12,13]. Therefore, estimation on the purity of fucoidan extracts become critical to the quality control point of view. However, the chemical composition of fucoidan extracted from brown seaweeds varies from species to species [6]. For example, isolated fucoidan from Fucus vesiculosus mainly consists of a relatively simple structure of fucose and sulphate (i.e., 1,2-α-fucose or 1,3- α-fucose and most of sulphate groups were located at position C-4 of the fucose) [3,14], while the chemical compositions of most fucoidan from other species are rather complex, including fucose, sulphate, other monosaccharides, uronic acids, and acetyl groups, etc. [6].

Previous publications on the research of fucoidan mainly dedicated in isolation techniques [1,15,16], elucidation of chemical structures [3,9,[17], [18], [19]], compositional analysis and bioactivity studies [1,5,6,12,20,21]. Admittedly, all these researches exploited specific fucoidan characteristics from many aspects; whereas, very few studies investigated on the development of direct analytical methods for purity determination of fucoidan mostly due to that there hasn't been unanimous agreement on the definite structure of fucoidan yet [18,20]. Some estimation methods were based on the estimation of common chemical features (e.g., fucose, sulphated polysaccharides, fuco-oligosaccharides) of fucoidan. A spectrophotometric method was developed to quantitatively determination of fucoidan content in a sample based on the quantification of its fucose content, which was multiplied by two; it is assumed that the average fucose content accounts for 50% of

fucoidan content [22]. A cationic dye method based on UV–visible spectral information at 520, 544 or 632 nm was used to quantify sulphated polysaccharides as the indicator of fucoidan content [23]. Sulphated polysaccharides content was also determined using 1H NMR; quantification based on molecular weights was potentially carried out using gel filtration chromatography or mass spectroscopy [7,8]. L-fucopyranose rings in oligosaccharides of fucoidan chains were investigated using 13C NMR for predictive modelling [4]. High performance liquid chromatography (HPLC) analysis of the acid hydrolysates with precolumn derivatization was used to determine the distribution of fucoidan-rich polysaccharide fractions with crude sodium alginate extract and final residue fractions of the acidic extract from brown seaweed species [24].

Vibrational spectroscopy (i.e., FT-IR and Raman) hold great potential for quantitative analysis of biopolymers. FT-IR spectroscopy has been employed for the chemical structure analysis on fucoidan isolated from brown seaweeds in many studies [1,9,16,17,19,20]. Whereas the limited utilities of FT-IR technique in transmittance mode were mainly on the detection of chemical functional groups and striking spectral features. Attenuated total reflectance (ATR)-FT-IR coupled with multivariate data analysis was reported to discriminate agave fructan adulterated fucoidan in powder mixtures (0–100%) and demonstrated the linear regression between FT-IR spectral data and the fucoidan content ($R2 \geq 0.92$ and RMSE $\leq 3.54\%$) [25]. Raman spectroscopy is even more rarely mentioned for the research of fucoidan due to the complicities of its Raman spectral features. Some study explored the Raman spectra of fucoidan that carried in acid solutions and illustrated the variations of Raman spectra that collected at different time points [26]. Both Raman and FT-IR spectroscopy are non-invasive and non-destructive techniques for real time routine analysis; in addition, Raman spectroscopy has considerable advantages in analysis of drug crystalline phases; compared with FT-IR, this technique is more sensitive to detect polymorphic forms of drugs with detailed spectral information of trace elements in situ with high resolution [[27], [28], [29]]. Besides, chemometrics can be applied to extract information from these spectroscopic systems by data-driven means for descriptive and predictive approaches.

Therefore, the current study investigated to develop analytical tools based on FT-IR or Raman spectroscopy and chemometrics for the purity determination of fucoidan isolated from brown seaweed species. Comparisons of vibrational spectroscopic methods with the other two wet chemistry methods and a HPLC method were also carried out to discuss the potentiality of all these methods for fucoidan purity determination.

2. Materials and methods

2.1. FT-IR and Raman spectroscopy with chemometrics on solid fucoidan samples

2.1.1. Solid sample preparation

Fucoidan from Fucus vesiculosus (≥95% purity) (CAS no.9072-19-9, Sigma-Aldrich, St. Louis, MO, USA) and KBr (CAS no.7758-02-3, Sigma-Aldrich, St. Louis, MO, USA) were dissolved in distilled water (10 ml) for the preparation of sample solutions (Table 1). Two replicates were carried out for the preparation of each sample formula. Sample solutions were frozen and then freeze-dried into fine powder using a freeze dryer (FD 80 model, Cuddon Engineering, Blenheim Marlborough, New Zealand) for 36 h. The powder of each sample (0.5 g) was compressed into a pellet using a 15-ton hydraulic press (Specac Ltd., Orpington, UK). Solid pellet samples for prediction model developments were prepared to include fucoidan purity levels of ca. 10%, 20%, 40% and 100%. Four commercial fucoidan samples (with detailed product information shown in Table 2) were also compressed into pellets for both FT-IR and Raman measurements.

Table 1. Formulations of fucoidan and KBr solutions prepared for pellet samples that used for FT-IR and Raman measurements.

Sample formulation	Fucoidan (g)	KBr (g)	Distilled water (ml)	Estimated fucoidan purity levels in dried mixtures (% mass/mass)
1	0.05	0.45	10	~10
2	0.1	0.40	10	~20
3	0.2	0.30	10	~40
4	0.5	0	10	~100

Table 2. Commercial fucoidan samples used for validation.

Commercial samples	Information of commercial samples	Sources
Commercial A	Confidential	*Undaria pinnatifida*
Commercial B	Confidential	*Undaria pinnatifida*
Commercial C	Confidential	*Fucus vesiculosus*
Sigma Crude	CAS no. 9072-19-9, Sigma-Aldrich Ltd., USA	*Fucus vesiculosus*

2.1.2. FT-IR measurements

FT-IR spectra of the pellet samples were collected using Nicolet™ iS5 (Thermo Scientific, Madison, WI, USA) Fourier transform mid-infrared spectrometer equipped with diamond crystal attenuated total reflectance (ATR) accessory (iD7 ATR, Thermo Scientific, Madison, WI, USA). Single beam reflectance spectra were recorded in the wavelength range of 550–4000 cm−1 with a resolution of 4 cm−1. Background calibration was carried out using air blank reference before each measurement. During each measurement, 64 scans were performed and averaged. Spectral data were recorded using the supplied OMNIC software v 9.2.98 (Thermo Fisher Scientific Inc., USA). Each sample was measured in triplicate and the mean value was acquired for chemometric analysis.

2.1.3. Raman measurements

Raman spectroscopic measurements were carried out using a DXR Smart Raman spectrometer (ThermoFisher Scientific UK Ltd., Loughborough, UK) equipped with a diode laser operating at 780 nm and a charge coupled device (CCD) detector. Samples were scanned at ambient temperature (ca. 20 °C) in a random order. The sample pellet was placed on the aperture (50 µm slit) of the universal platform sampling accessory. The spectra of each sample were collected in 5 min (i.e., 15 s exposure time × 20 exposures) using a 150 mW laser power. Raman intensity counts per second (cps) were recorded over the wavelength range 450–3380 cm−1 at 4 cm−1 intervals. Instrument control, spectral acquisition, cosmic spikes removal and file conversion were performed using the supplied OMNIC software v 9.2.98 (Thermo Fisher Scientific Inc., USA). Each sample was scanned twice on each side of the sample pellet, respectively; the mean of these duplicate spectra was used in subsequent chemometric analysis.

2.1.4. Multivariate data analysis on FT-IR and Raman spectra

Spectral data was exported from OMNIC software as .csv files and imported into MATLAB 2019a (The Mathworks, Natick, MA, USA). Baseline correction on raw data was carried out using asymmetric least squares correction (AsLs). Based on the intensities of both FT-IR and Raman spectral variables, the selected wavelength ranges (i.e., 550–1800 cm−1 of FT-IR and 550–3060 cm−1 of Raman spectra) were selected and used as the X-variables, respectively; and the estimated fucoidan purity levels (i.e., 10%, 20%, 40% and100%) shown in Table 1 were used as the Y-variables (reference values) for the development of partial least squares regression (PLSR) models. PLSR models were developed using the nonlinear iterative partial least squares (NIPALS) algorithm on the spectral data of the calibration samples (i.e., the prepared pellet samples (n = 8)). Robustness of the PLSR model was enhanced using the most relevant spectral variables which were selected using

variable importance on projection (VIP) and selectivity ratio (SR) algorithms for FT-IR and Raman spectral data, respectively [30,31]. Leave-one-out cross-validation was carried out to validate the developed models. These models were also validated using the FT-IR and Raman spectral data of the four commercial samples, respectively. The performance of PLSR modelling was evaluated using regression coefficient of determination of calibration (R2C), cross-validation (R2CV) and prediction (R2P) with their corresponding root mean square error values (RMSEC, RMSECV and RMSEP) and bias. The regression coefficient of determination (R2) is a statistical value to explain the relationship of Y-variables and X-variables in percentage of variations; the root mean square (RMSE) values calculated is to describe the standard prediction errors with bias of the cross-validation/validation results. For a model with high prediction accuracy, the R2 values are expected to be close to 1; and the RMSEs and bias are expected to be close to 0. R2, RMSE, and bias were calculated following the equations as below:

$$R^2 = 1 - \frac{\sum_{i=1}^{n} \left(\hat{y}_i - y_i\right)^2}{\sum_{i=1}^{n} \left(\hat{y}_i - \bar{y}\right)^2} \quad (1)$$

$$RMSE = \sqrt{\frac{\sum_{i=1}^{n} \left(y_i - \hat{y}_i\right)^2}{n}} \quad (2)$$

$$Bias = \frac{\sum_{i=1}^{n} y - \hat{y}_i}{n} \quad (3)$$

where $\hat{y}_i$ is the predicted value and y_i is the reference value of a sample (*i*); $\bar{y}$ is the mean of the reference values of all the samples.

2.1.5. Limits of detection (LOD)

The limit of detection (LOD) values of the developed PLSR models were calculated. LOD is the smallest content or concentration of an analyte in the test sample that can be reliably distinguished by a developed model. Therefore, the LOD value of an ideal model is expected to be as low as possible. Pseudo-univariate LOD (LODpu) concerns with the uncertainty of the calibration line and the considered errors. The international union of pure and applied chemistry (IUPAC) recommended LOD formula as below:

$$LOD_{pu} = 3.3\, s_{pu}^{1}[(1 + h_{0\ min} + 1/I)\, var_{pu}]^{\frac{1}{2}} \quad (4)$$

where spu−1 is the slope of the pseudo-univariate line, h0 min is the minimum leverage when the concentration of analyte is 0, I is the number of samples, varpu is the variance of the regression residual [32].

2.2. Chemical methods for fucoidan estimation

The chemicals used here including toluidine blue, maleic acid (≥ 99%), sulfuric acid (95–97%), L-cysteine hydrochloride, fucoidan from Fucus vesiculosus (≥ 95%) and L-(-)-fucose (≥ 99%) were purchased from SIGMA (Sigma-Aldrich, St. Louis, MO, USA). All other reagents used were of analytical grade.

2.2.1. Fucoidan estimation based on fucose content

Fucoidan contents were estimated by performing fucose measurements as described by Dische and Shettles (1948) [33]. Briefly, 1 mL of fucose standards (ranging from 0.005 to 0.1 mg/ml) and macroalgal extracts at appropriate dilutions were added to 4.5 mL of a sulfuric acid solution (1:6, water:sulfuric acid), incubated for 10 min at 100 °C in a water bath and cooled to room temperature. Afterwards, 0.1 mL of a L-cysteine hydrochloride solution (3% w/v) were added into the solution and incubated for 60 min at room temperature. Then the absorbance of the reactions was read at 396 nm and 430 nm in a spectrophotometer (Epoch™ 2, Biotek, VT, USA). The standard fucose concentrations were used to against the absorbance of 396 nm and 430 nm to develop a linear correlation. The level of fucose in fucoidan polysaccharides constitutes 50% on average; thus, the values of fucoidan were estimated from the fucose values by using a conversion factor of 2 as previous studies have applied when working with macroalgal extracts [22,34]. The commercial samples were also dissolved in distilled water in 0.1 or 0.25 mg/ml and read at 396 nm and 430 nm for absorbance values. All analyses were performed in duplicate with 3 readings of each replica (n = 6). The fucoidan content of the samples was expressed as mg fucoidan/100 mg sample (%).

2.2.2. Fucoidan estimation using cationic dyes

The amount of fucoidan in the samples was estimated using a cationic dye method to measure sulphated polysaccharides [23]. Briefly, 16 µl of fucoidan standards (0.1–1.5 mg/ml) or commercial sample solutions (0.1 or 0.25 mg/ml) at appropriate dilutions were assayed by adding 1584 µl of a toluidine blue solution at pH 1 (0.06 mM toluidine blue dye in 0.02 M maleic acid) and mixed thoroughly; the absorbance of the reactions was read at 632 nm in a spectrophotometer (Epoch™ 2, Biotek, VT, USA). A correlation was developed between the concentrations of fucoidan standards and the absorbance values at 632 nm. All analyses were also performed in duplicate with 3 readings of each replica (n = 6). The results are expressed as mg fucoidan per 100 mg of sample (%).

2.3. High performance liquid chromatography refractive index detector (HPLC-RI) for fucoidan estimation

Fucoidan was separated and quantified from the samples using a HPLC system (LC-20AT, Shimadzu North America, Columbia, MD, USA), fitted with a refractive index detector VARIAN Pro Star 350 (Varian Inc., Mulgrave, Victoria, Australia) and a SUPELCOGEL™ C610H with 6% crosslinked HPLC carbohydrate column with 300 mm × 7.8 mm (length x I.D.) and 9 µm of particle size (Sigma-Aldrich, Bellefonte, PA, USA). All samples were diluted to 2 mg/ml and filtered through 2 µm filters (Whatman, Buckinghamshire, UK) and 10 µl were injected using an auto sampler (SIL-20 AC HT, Shimadzu North America, Columbia, MD, USA). The separation was achieved by using 0.1% phosphoric acid as a mobile phase at a constant flow rate (0.5 ml/min, 20 min) and 30 °C of column temperature. The identification of fucoidan was performed by comparison of the retention times with those of fucoidan standard from Fucus vesiculosus (≥95% purity) (CAS no.9072-19-9, Sigma-Aldrich, St. Louis, MO, USA). The integration of the peaks was performed using the software (LabSolutions, Shimadzu North America, Columbia, MD, USA). The correlation between fucoidan concentrations and peak areas were developed. All the analyses were performed in duplicate and the fucoidan content expressed as mg per 100 mg sample (%).

2.4. Statistical analysis on fucoidan estimation of the analytical methods

The estimated fucoidan content (%) of the four commercial samples using individual analytical technique were expressed as the predicted value ± RMSEP for the FT-IR and Raman spectroscopic/chemometric methods; mean ± standard deviation for the chemical methods and the HPLC-RI method. One-way analysis of variance (ANOVA) was performed on the estimation results of each sample using Post Hoc with Tukey's HSD test to determine the significance ($p \leq 0.05$) between the estimated results of the analytical methods used.

3. Results and discussion

3.1. Results of FT-IR and Raman

Baseline corrected FT-IR spectra (550–4000 cm−1) of the calibration samples (n = 8) were shown in Fig. 1a. It can be observed that two obvious absorbance bands existing at 2930 cm−1 and 3441 cm−1, which were the most common spectral features that assigned to Csingle bondH and Osingle bondH stretching of polysaccharides [35]. The fingerprint region of FT-IR spectra for fucoidan determination was in the wavelength range of 550–1800 cm−1 (Fig. 1b). The absorption intensities of these spectra depict in an increased trend following the fucoidan content levels of 10, 20, 40 and 100%. Absorption bands around 573–579 cm−1 were related to Ssingle bondO stretching vibration [9,36]; the strong bands at 836–840 cm−1 and 1228–1256 cm−1 were related to C-O-S bending vibration of sulphate substituents at the axial C-4 position and Sdouble bondO stretching, respectively [20,36]; other bands at 1132 and 1166 cm−1 indicate the presence of Sdouble bondO stretching of alkyl sulfoxide [1]; 960–964 cm−1 were assigned to the asymmetric and symmetric deformation vibrations of methylidyne in fucose [20,35]; bands at 1006–1026 cm−1, 1050 cm−1 and 1079 cm−1 were related to Csingle bondC and C-O-C stretching of carbohydrate [35]; 1639–1649 cm−1 might be related to Cdouble bondO of a carboxylic acid group (-COOH) and vibrations of crystalized water [1,20].

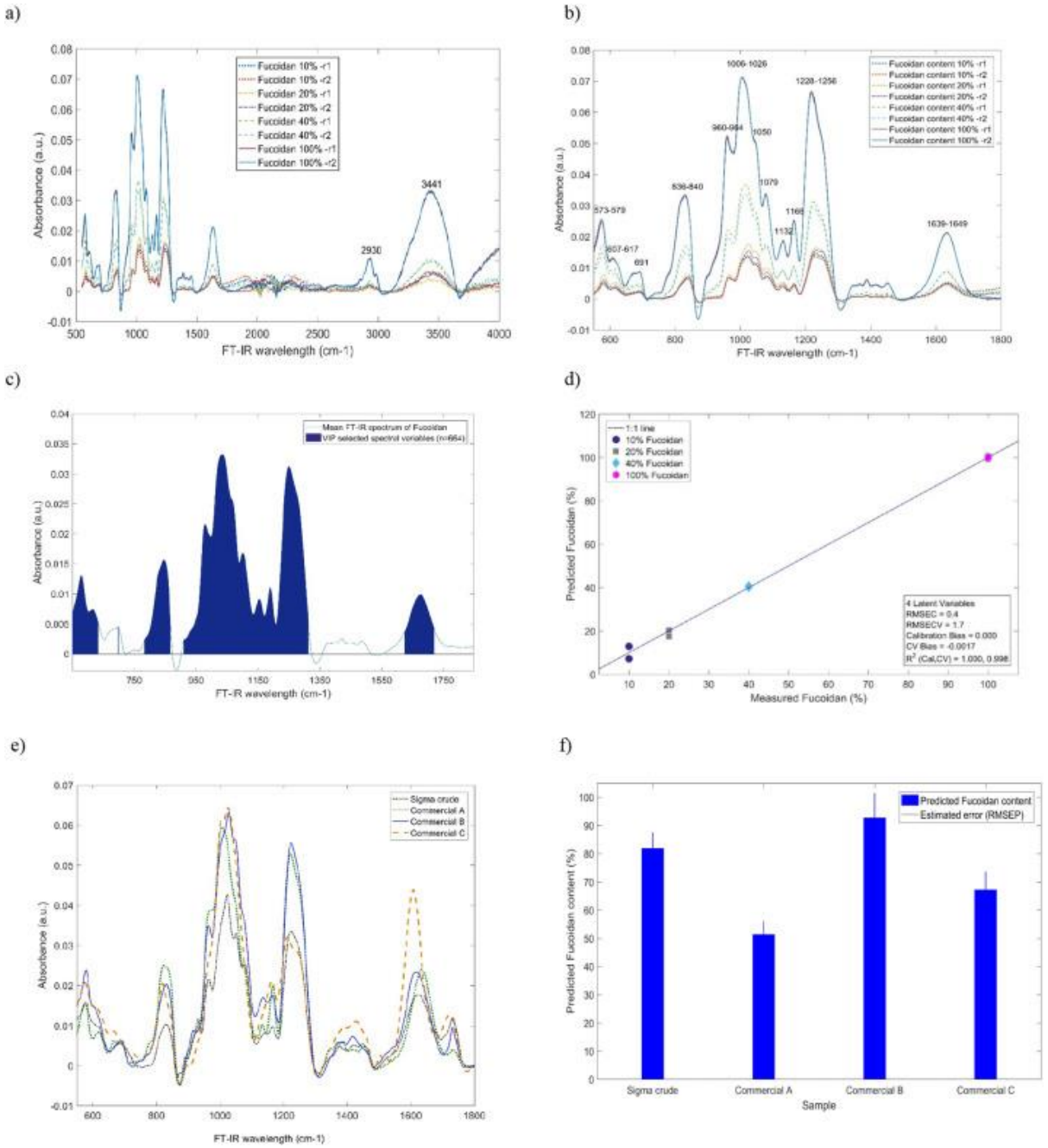

Fig. 1. a). AsLs baseline corrected FT-IR spectra (550–4000 cm−1) of fucoidan samples in the calibration group (n = 8); b) AsLs baseline corrected FT-IR spectra (550–1800 cm−1) of fucoidan samples in the calibration group (n = 8); c) mean FT-IR spectrum (550–1800 cm−1) highlighted with the VIP selected spectral variables; d) the plot of PLSR model developed using VIP selected spectral variables in 550–1800 cm−1; e) AsLs baseline corrected FT-IR spectra (550–1800 cm−1) of the commercial fucoidan samples (n = 4); f) bar plot of predicted fucoidan contents and the estimated errors of the commercial fucoidan samples (n = 4).

PLSR modelling was initially carried out using the FT-IR spectral variables (n = 1298) of 550–1800 cm−1 and obtained the regression coefficient determinations of calibration (R2C) of 0.999 and cross-validation (R2CV) of 0.990 with the root mean square errors of cross-validation (RMSECV) of 3.4% and bias of 0. The PLSR model was also carried out using the VIP algorithm to select spectral variables (n = 664), which were highlighted on the mean FT-IR spectrum over 550–1800 cm−1 (Fig. 1c). VIP algorithm was implemented to accumulate the importance of each spectral variable that can be reflected by the loading weights of each latent component that derived from PLSR modelling [37]. The PLSR model developed using the VIP selected spectral variables (n = 664) also revealed R2C of 1 and R2CV of 0.998 with the RMSECV of 1.7% and bias of 0 (Fig. 1d). Therefore, it can be identified that the spectral features that may related to fucoidan chemical structures were included in the VIP selected spectral bands, especially in the wavelengths of 573–579, 836–840, 900–1300 and 1639–1649 cm−1. The spectra of four commercial fucoidan samples were collected and shown in Fig. 1e; the spectral features of these four commercial samples were almost the same to those of fucoidan samples for model calibration in the VIP selected spectral wavelengths. To validate the developed PLSR model, fucoidan purities (%) of the four commercial samples were predicted using the PLSR model and revealed R2P of 0.978 and RMSEP of 6.7%. In Fig. 1f, the predicted fucoidan contents and the corresponding estimated errors (RMSEP) are shown as 81.93% ± 5.64% for Sigma crude, 51.44% ± 4.61% for Commercial A, 92.74% ± 8.05% for Commercial B and 67.27% ± 6.34% for Commercial C. The LOD of the PLSR model was 2.66%.

Fig. 2a shows the AsLs baseline corrected Raman spectra (450–3380 cm−1) of the calibration sample group (n = 8) and the KBr pellet samples (n = 2). The spectra of KBr are general flattened with the Raman spectral intensity count per second (cps) close to 0, especially in the frequency range of 550–3060 cm−1. It demonstrated that KBr contained in the pellets of calibration samples would not interfere the Raman spectral features of fucoidan content during Raman spectral measurements. The Raman spectra of the calibration sample group laid out following the logic order of fucoidan content levels from 10% to 100% in most of the spectral range of 550–3060 cm−1, while the two ends of the spectra were scattered out. In Fig. 2b, some very weak spectral bands at 581 cm−1 and 656 cm−1 are assigned to pyranose ring breathing and Osingle bondH wagging deformation; bands at 826, 882 and 1053 cm−1 are all related to C-O-C deformation of glycosidic linkage; 1053 cm−1 and 1123 cm−1 are both related to Csingle bondO vibration, 1053 cm−1 and 1123 cm−1 are also related to Csingle bondC vibration and C-C-H deformation [38]. The region around 1060 cm−1 is also assigned to the Sdouble bondO symmetric vibration of sulphate content [39]. Some strong and medium strong bands at 1273, 1331 and 1452 cm−1 are assigned to C-O-H deformation; 1273, 1331, 1400 and 1452 cm−1 are related to Csingle bondH deformation of polysaccharides [38]. A strong

band at 2947 cm−1 is assigned to Csingle bondH stretching vibration of polysaccharides [35]. During the PLSR modelling using all the spectral variables (n = 2085) in the Raman frequency range of 550–3060 cm−1, the SR algorithm was implemented to select the most important spectral variables that related to fucoidan content, which were selected based on the calculated SR scores of all the spectral variables used for modelling; the SR scores that defined by the ratio between the explained and unexplained variances for each spectral variable were calculated using both the predictive ability (regression vector) and the explanatory ability (spectral variance/covariance matrix). The boundary between variable regions with high discriminating ability and less interested regions was identified using F-test to decide the critical value of the F distribution with 95% confidence. Therefore, the SR selected spectral variables (n = 563) were highlighted on the mean spectrum of fucoidan samples in the calibration group (Fig. 2c); most of the selected spectral variables were in the range of 550–2000 cm−1 and 2905–2969 cm−1.

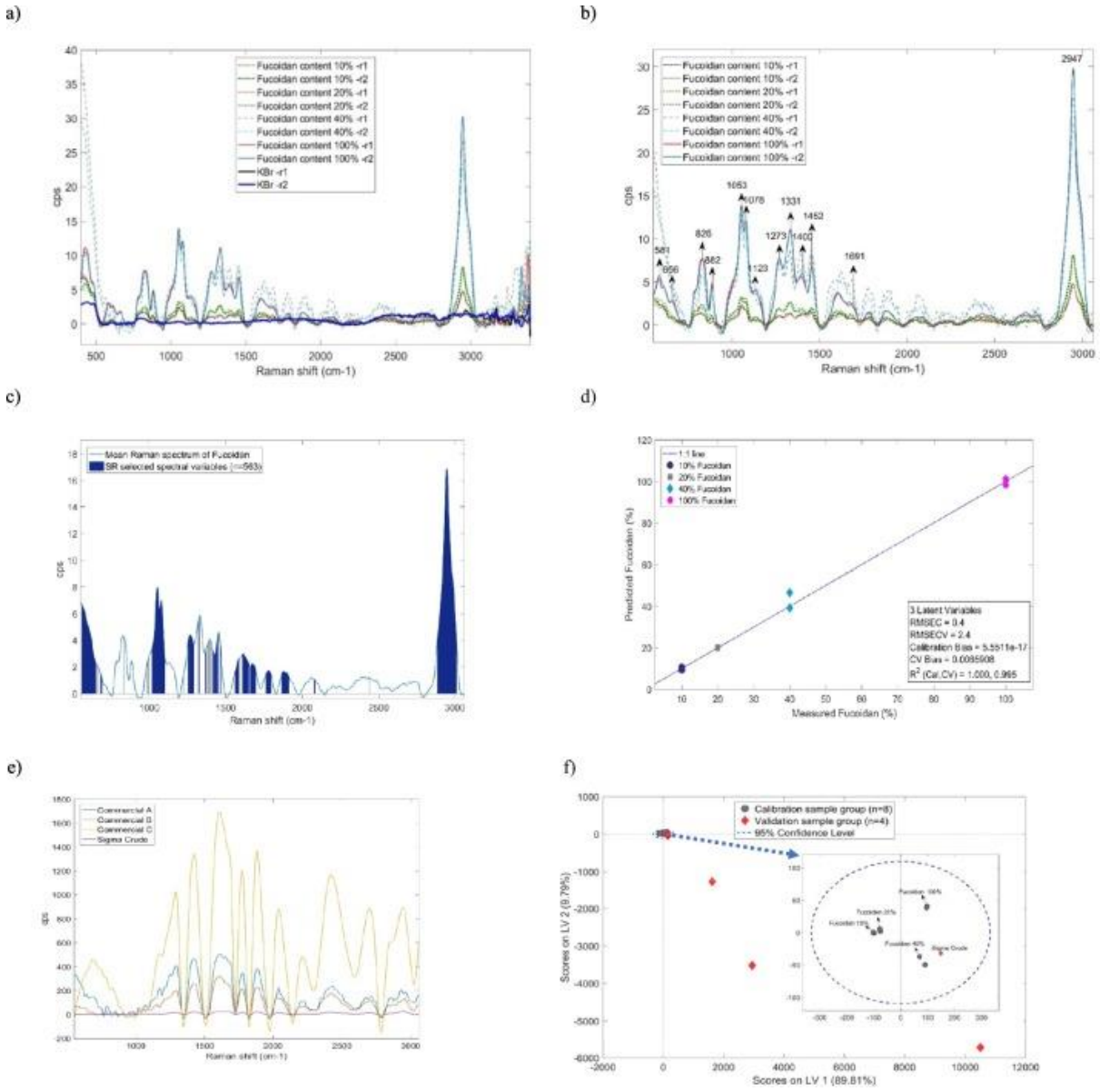

Fig. 2. a). AsLs baseline corrected Raman spectra (450–3380 cm−1) of fucoidan samples in the calibration group (n = 8) and KBr samples (n = 2); b) AsLs baseline corrected Raman spectra (450–3060 cm−1) of fucoidan samples in the calibration group (n = 8); c) mean Raman spectrum (450–3060 cm−1) highlighted with the SR selected spectral variables; d) the plot of PLSR model developed using SR selected spectral variables in 450–3060 cm−1; e) AsLs baseline corrected Raman spectra (450–3060 cm−1) of the commercial fucoidan samples (n = 4); f) PLS score plot (LV1 vs. LV2) of the samples in the calibration group (n = 8) and the validation group (n = 4).

The PLSR model developed using all the baseline corrected Raman spectral variables (n = 2605) in 550–3060 cm−1 of the calibration group obtained R2C of 0.999 with RMSEC of 1.08%, R2CV of 0.989 with RMSECV of 3.68%; three latent variables (LVs) were included in the PLSR modelling. Based on the SR selected spectral variables (n = 563), the developed PLSR model revealed R2C of 1with RMSEC of 0.87% and R2CV of 0.994 with RMSECV of 2.96%; the bias of calibration is 0 and that of cross-validation is 0.0065 (0.65%) (Fig. 2d). The model was also used to predict the fucoidan content of the four commercial samples. However, it can be observed in Fig. 2e that Raman spectra (550–3060 cm−1) of the commercial samples with much higher scatter light intensity (cps) than those of the calibration samples (Fig. 2b) except the Sigma Crude sample. The PLS score plot in Fig. 2f also depicts that the clustering of the calibration samples and the Sigma Crude sample, which were located in the ellipse of the Hotelling's T2 at 95% confidence level; the other three commercial samples were not included in the ellipse. Thus, only the fucoidan content of the Sigma Crude sample can be predicted by the PLSR model as 75.21% ± 12.44%. The LOD of the PLSR model is 3.19%.

3.1.1. Discussion on FT-IR and Raman spectroscopy with chemometrics for the determination of fucoidan purity

In the current study, PLSR models for purity determination of fucoidan extracted from brown seaweed species were developed on both FT-IR and Raman spectral data of the prepared samples with fucoidan content levels at 10%, 20%, 40% and 100%. The commercial fucoidan product with the labelled purity (≥95%) was assumed to be fucoidan content of 100%, and other fucoidan content levels were prepared based on the same assumption. Thus, the latent error (≤5%) should also be accounted as the additional part to the estimated errors that derived from PLSR modelling.

Both FT-IR and Raman spectra of the collected wavelength ranges contain complex information of the sample matrices, which includes the relevant chemical structures of fucoidan and other chemical structures of the impurities contained in the measured samples. VIP and SR algorithms were investigated to select the most relevant spectral variables of fucoidan and eliminate the variables related to other impurities. Therefore, the PLSR models developed using VIP or SR selected spectral variables demonstrated more robustness (with higher R2 values and lower RMSE values) than those developed using all the spectral variables in the selected wavelength ranges.

Normally, Raman spectral data acquisition is interfered by florescence effects while FT-IR spectra can be influenced by carbon dioxide existing in air during the measurements. Hence the AsLs baseline correction was used to remove these interferences on spectra but to remain most of original

spectral features. In this study, Raman spectral shape and intensity of the scatter light counts per seconds (cps) were found to be prone to reflect the polymorphic forms of these commercial samples, which were possibly produced under different purification and crystalline processes; it can be observed that the Raman spectra of the commercial samples (Fig. 2e) (except the Sigma Crude sample) were quite different from the calibration samples that prepared using fucoidan (≥95% purity) (CAS no.9072-19-9, Sigma-Aldrich, USA) (Fig. 2b). Therefore, only the Sigma Crude sample can be predicted by the PLSR model developed using the calibration samples. Since the sample materials were compressed into pellets and then analysed, the compression induced solid-state transitions of the substance [27]; Raman spectroscopy is still excellent to discriminate different polymorphs and pseudo-polymorphs of substance [40], while FT-IR spectroscopy seems to be less sensitive to determine particle surface morphology after the solid-state transitions by compression [27]. Instead of that, FT-IR spectral features of chemical compositions were enhanced. The PLSR model developed using FT-IR spectral data demonstrated potential on the determination of fucoidan purity and obtained a higher R2CV value (R2CV = 0.998), a lower RMSECV value (RMSECV = 1.7%) and a lower LOD value (LOD = 2.66%) than those (R2CV = 0.995, RMSECV = 2.4%, LOD = 3.19%) of models developed using Raman spectral data. In general, the FT-IR spectroscopic method with chemometrics demonstrated higher prediction accuracy and sensitivity for the determination of fucoidan content than the Raman spectroscopic method.

3.2. Results and discussion of chemical methods for fucoidan estimation

The fucose content of the samples was determined against the fucose standard at effective absorbance of 396 nm and 430 nm with the linearity (R2 = 0.993). Fucoidan estimation was performed on the four commercial samples. Each sample was prepared in duplicate and measured in triplicate; therefore, the averaged fucoidan concentration and the standard deviation were calculated from six estimated concentrations. The fucoidan contents of the samples expressed as average ± standard deviation of the mean based on the measurement of fucose were 63.07 ± 0.47%, 34.97 ± 0.22%, 75.85 ± 0.58% and 35.06 ± 0.40% for Sigma Crude, Commercial A, Commercial B and Commercial C samples, respectively. The spectrophotometric determination of fucoidan on the basis of fucose content is currently considered as the most simple and reliable method to determine fucoidan, as the possible interference of other sugars to the colour of this reaction is excluded by the colour measurements at 2 different wavelengths [22]. The determination of fucoidan on the basis of fucose is widely used to estimate the fucoidan content of macroalgae and macroalgal extracts to date [34,41]. Limitations of this method are mainly related to the colour of the samples, as the analyses can be difficult to apply if the fucoidan samples contain more pigments. The precipitation of

fucoidan with ethanol containing magnesium salts has been proposed as a sample pre-treatment to eliminate pigments from the samples [22]. However, the application of this pre-treatment is often ineffective and complicates substantially the procedures for fucose estimation [22]. Therefore, the estimation values of Commercial A (34.97 ± 0.22%) and Commercial C (35.06 ± 0.40%) were lower than that expected due to their high pigment contents, which can be visually identified.

For the cationic dye method, the linear correlation of absorbance at 633 nm and fucoidan concentrations (mg/ml) was developed with R2 of 0.997. Each sample was also prepared in duplicate and measured in triplicate. The fucoidan content levels (mean ± standard deviation) of the four commercial samples were estimated as 69.17 ± 0.37% for Sigma Crude, 61.70 ± 0.31% for Commercial A, 108.56 ± 0.13% for Commercial B, and 26.32 ± 0.22% for Commercial C. The dye method is a recently established method to determine the fucoidan content using toluidine blue [23]. The adsorption of the dye to the polysaccharides namely metachromasia results in a charge-transfer-complex, which is detected using UV/Vis-spectroscopy. Metachromatic dyes such as methylene blue and ortho-toluidine blue with high molar attenuation coefficients and pronounced spectral shifts are currently used to develop fast and simple spectrophotometric methods to analyse sulphated containing polysaccharides including carrageenan [42,43] and fucoidan [23]. The advantages of this spectrophotometric method using dyes are the minimal preparation procedures as well as the affordable instrumentation needed [43]. The interferences of the dye with other polyanionic groups from other molecules (i.e., alginates and DNA) were eliminated by acidifying the pH of the dye, inducing a protonation of interfering molecules [23]. However, the main limitation of this method is the susceptibility to form precipitates with polyanionic analytes resulting in signal disturbances [43] that takes place at certain dye-to-polymer ratios when all the anionic moieties are saturated with dye cations [44]. Furthermore, this method used provides only an estimation of sulphated polysaccharides in the samples [23] and thus, the presence of other sulphated polysaccharides, such as carrageenan, may result in an overestimation of fucoidan content when using this method alone. It was noticed that overestimation of fucoidan content (108.56 ± 0.13%) for Commercial B happened in this study.

3.3. Results and discussion of HPLC-RI

The content of fucoidan in the samples was determined against a fucoidan standard (≥ 95% purity) at effective concentrations of 0.1–2 mg/ml that showed a main peak at retention time (RT) of 9.1 min (Fig. 3a) with a linearity of R2 = 0.9997 (Fig. 3b). The analysis of the samples revealed the presence of fucoidan with prominent peaks at RT ranging from 9.1–9.2 min together with other non-identified peaks from impurities or non-identified compounds. Considering a standard purity of 95%

as estimated by Sigma, the concentration of fucoidan in the samples (average ± standard deviation of the mean) was 94.05 ± 0.24% for Sigma Crude, 49.50 ± 0.03% for Commercial A, 82.35 ± 0.12% for Commercial B, and 66.77 ± 0.85% for Commercial C. Chromatographic techniques, including HPLC-RI are widely used for a qualitative and quantitative determination of different carbohydrates with minimum sample pre-treatments. HPLC techniques for carbohydrate analysis have recently expanded and evolved due to advances in equipment and column packaging materials [45]. The column of this study (C610H, SUPELCOGEL™, Sigma-Aldrich, Bellefonte, PA, USA) is packed with polystyrene divinylbenzene co-polymers (PS-DVB) in a hydrogen form, allowing the separation of mixtures of organic acids and carbohydrates by eluting large and acidic analytes before small analytes [46]. RI is a universal detector and has a wide linear range at several carbohydrate concentrations that can be detected without the use of any derivatization technique [45,46]. However, the major disadvantages of this detector include a poor sensitivity of the method, the presence of both positive and negative peaks and baseline instability, being not suitable for gradient elution [46].

a)

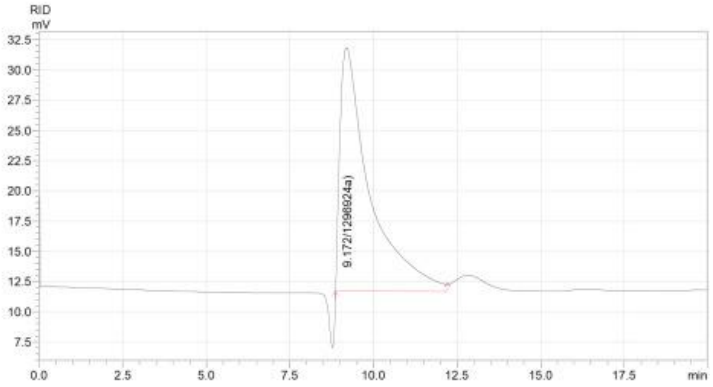

b)

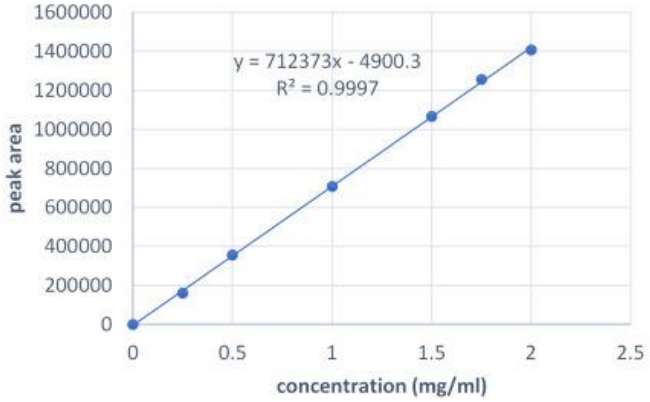

Fig. 3. a) HPLC chromatogram of standard fucoidan (≥95% purity, CAS no.9072-19-9, Sigma-Aldrich, St. Louis, MO, USA) separated on Supelcogel C610H. RT = 9.1 min; b) Fucoidan standard curve of concentration (mg/ml) vs. peak area.

3.4. Comparison of analytical methods based on the estimated fucoidan purity of commercial samples

A summary of statistical results on the estimated fucoidan content (%) of the four commercial samples by using the analytical methods (i.e., FT-IR, Raman, Fucose-method, Dye-method, and HPLC-RI) was shown in Table 3. The estimation values of Commercial A and C obtained from the Fucose-method were significantly lower than the values estimated by the FT-IR or the HPLC-RI method; and the estimated values of Commercial B or Commercial C obtained from the Dye-method were significantly higher or lower than the other estimated values of the same sample. On the other hand, there was no significant difference ($p > 0.05$) found between the fucoidan content values (of the same sample) that estimated by the FT-IR method or the HPLC-RI method. Thus, the reliability of these two methods on fucoidan content estimation was accordingly demonstrated by their similar estimation results of the same samples. The FT-IR spectroscopic method with chemometric investigated in the current study could be potentially used for non-destructive and real time determination on the purity of fucoidan extracted from seaweeds.

Table 3. Fucoidan content (%) of the commercial fucoidan samples estimated by the analytical methods used.

	Commercial A	**Commercial B**	**Commercial C**	**Sigma Crude**
FT-IR	51.44 ± 4.61^{b}	92.74 ± 8.05^{a}	67.27 ± 6.34^{b}	81.93 ± 5.64^{a}
Raman	–	–	–	75.21 ± 12.44^{a}
Fucose-method	34.97 ± 0.22^{a}	75.85 ± 0.58^{a}	35.06 ± 0.40^{a}	63.07 ± 0.47^{a}
Dye-method	61.17 ± 0.37^{b}	108.56 ± 0.13^{b}	26.32 ± 0.22^{a}	69.17 ± 0.37^{a}
HPLC-RI	49.5 ± 0.03^{b}	82.35 ± 0.12^{a}	66.77 ± 0.85^{b}	94.05 ± 0.24^{a}

Values in the same column with different letters are significantly different ($p \leq 0.05$).

4. Conclusions

In the current study, FT-IR and Raman spectroscopy combined with chemometric analysis were investigated to develop PLSR models for the determination of fucoidan purity. Compared to Raman spectroscopy, FT-IR demonstrated more potential to approach non-destructive prediction on fucoidan content of pellet samples that directly compressed from powdered fucoidan products. The developed prediction models were validated using the spectral information of four commercial samples with reasonable prediction results. Other two widely used chemistry analytical methods and the HPLC-RI method were also implemented to estimate fucoidan purity of the four commercial samples. Based on the estimation results, the pros and cons of all the analytical methods were discussed. The estimated fucoidan content results of the commercial samples using the FT-IR spectroscopic method were close to the estimated results using the HPLC-RI method. It can be concluded that it is possible to achieve quantitative determination of fucoidan content using data engineering and mathematical modelling on FT-IR spectral data, instead of the wet chemistry related analytical methods.

Acknowledgements

This study was financially supported by BEACON SFI Bioeconomy Research Centre, which is funded by Ireland's European Structural and Investment Programmes, Science Foundation Ireland (16/RC/3889) and the European Regional Development Fund.

References

[1] S. Palanisamy, M. Vinosha, T. Marudhupandi, P. Rajasekar, N.M. Prabhu, Isolation of fucoidan from Sargassum polycystum brown algae: Structural characterization, in vitro antioxidant and anticancer activity., International Journal of Biological Macromolecules. 102 (2017) 405–412. https://doi.org/10.1016/j.ijbiomac.2017.03.182.

[2] R. V Usoltseva, S.D. Anastyuk, I.A. Ishina, V. V Isakov, T.N. Zvyagintseva, P.D. Thinh, P.A. Zadorozhny, P.S. Dmitrenok, S.P. Ermakova, Structural characteristics and anticancer activity in vitro of fucoidan from brown alga Padina boryana, Carbohydrate Polymers. 184 (2018) 260–268. https://doi.org/https://doi.org/10.1016/j.carbpol.2017.12.071.

[3] M.S. Patankar, S. Oehninger, T. Barnett, R.L. Williams, G.F. Clark, A revised structure for fucoidan may explain some of its biological activities., The Journal of Biological Chemistry. 268 (1993) 21770–21776.

[4] A.A. Grachev, A.G. Gerbst, N.E. Ustyuzhanina, V.B. Krylov, A.S. Shashkov, A.I. Usov, N.E. Nifantiev, Modeling of polysaccharides with oligosaccharides: how large should the model be?, Mendeleev Communications. 17 (2007) 57–62. https://doi.org/https://doi.org/10.1016/j.mencom.2007.03.001.

[5] A.S. Silchenko, A.B. Rasin, M.I. Kusaykin, A.I. Kalinovsky, Z. Miansong, L. Changheng, O. Malyarenko, A.O. Zueva, T.N. Zvyagintseva, S.P. Ermakova, Structure, enzymatic transformation, anticancer activity of fucoidan and sulphated fucooligosaccharides from Sargassum horneri, Carbohydrate Polymers. 175 (2017) 654–660. https://doi.org/https://doi.org/10.1016/j.carbpol.2017.08.043.

[6] B. Li, F. Lu, X. Wei, R. Zhao, Fucoidan: Structure and Bioactivity, Molecules. 13 (2008) 1671–1695. https://doi.org/10.3390/molecules13081671.

[7] S. Song, S. Wu, C. Ai, X. Xu, Z. Zhu, C. Cao, J. Yang, C. Wen, Compositional analysis of sulfated polysaccharides from sea cucumber (Stichopus japonicus) released by autolysis reaction, International Journal of Biological Macromolecules. 114 (2018) 420–425. https://doi.org/https://doi.org/10.1016/j.ijbiomac.2018.03.137.

[8] P.D. Thinh, B.M. Ly, R. V Usoltseva, N.M. Shevchenko, A.B. Rasin, S.D. Anastyuk, O.S. Malyarenko, T.N. Zvyagintseva, P.T. San, S.P. Ermakova, A novel sulfated fucan from Vietnamese sea cucumber Stichopus variegatus: Isolation, structure and anticancer activity in vitro, International Journal of Biological Macromolecules. 117 (2018) 1101–1109. https://doi.org/https://doi.org/10.1016/j.ijbiomac.2018.06.017.

[9] D. Leal, A. Mansilla, B. Matsuhiro, M. Moncada-Basualto, M. Lapier, J.D. Maya, C. Olea-Azar, W.M. De Borggraeve, Chemical structure and biological properties of sulfated fucan from the sequential extraction of subAntarctic Lessonia sp (Phaeophyceae), Carbohydrate Polymers. 199 (2018) 304–313. https://doi.org/https://doi.org/10.1016/j.carbpol.2018.07.012.

[10] C. Murphy, S. Hotchkiss, J. Worthington, S.R. McKeown, The potential of seaweed as a source of drugs for use in cancer chemotherapy, Journal of Applied Phycology. 26 (2014) 2211–2264. https://doi.org/10.1007/s10811-014-0245-2.

[11] H.-W. Park, D.-Y. Kim, W.-S. Shin, Fucoidan improves the structural integrity and the molecular stability of β-lactoglobulin, Food Science and Biotechnology. 27 (2018) 1247–1255. https://doi.org/10.1007/s10068-018-0375-4.

[12] A.M.S. Mayer, A.D. Rodríguez, R.G.S. Berlinck, N. Fusetani, Marine pharmacology in 2007–8: Marine compounds with antibacterial, anticoagulant, antifungal, anti-inflammatory, antimalarial, antiprotozoal, antituberculosis, and antiviral activities; affecting the immune and nervous system, and other miscellaneous mec, Comparative Biochemistry and Physiology Part C: Toxicology & Pharmacology. 153 (2011) 191–222. https://doi.org/https://doi.org/10.1016/j.cbpc.2010.08.008.

[13] T.-S. Vo, S.-K. Kim, Fucoidans as a natural bioactive ingredient for functional foods, Journal of Functional Foods. 5 (2013) 16–27. https://doi.org/https://doi.org/10.1016/j.jff.2012.08.007.

[14] J. Conchie, E.G. V Percival, 167. Fucoidin. Part II. The hydrolysis of a methylated fucoidin prepared from Fucus vesiculosus, Journal of the Chemical Society (Resumed). (1950) 827–832. https://doi.org/10.1039/JR9500000827.

[15] S.J. Lim, W.M. Wan Aida, M.Y. Maskat, S. Mamot, J. Ropien, D. Mazita Mohd, Isolation and antioxidant capacity of fucoidan from selected Malaysian seaweeds, Food Hydrocolloids. 42 (2014) 280–288. https://doi.org/https://doi.org/10.1016/j.foodhyd.2014.03.007.

[16] M.D. Hanjabam, A. Kumar, C.S. Tejpal, E. Krishnamoorthy, P. Kishore, K. Ashok Kumar, Isolation of crude fucoidan from Sargassum wightii using conventional and ultra-sonication extraction methods, Bioactive Carbohydrates and Dietary Fibre. 20 (2019) 100200. https://doi.org/https://doi.org/10.1016/j.bcdf.2019.100200.

[17] Y. Song, Q. Wang, Q. Wang, Y. He, D. Ren, S. Liu, L. Wu, Structural characterization and antitumor effects of fucoidans from brown algae Kjellmaniella crassifolia farmed in northern China, International Journal of Biological Macromolecules. 119 (2018) 125–133. https://doi.org/https://doi.org/10.1016/j.ijbiomac.2018.07.126.

[18] A.D. Holtkamp, S. Kelly, R. Ulber, S. Lang, Fucoidans and fucoidanases—focus on techniques for molecular structure elucidation and modification of marine polysaccharides, Applied Microbiology and Biotechnology. 82 (2008) 1. https://doi.org/10.1007/s00253-008-1790-x.

[19] N. Liu, X. Wu, X. Fu, D. Duan, J. Xu, X. Gao, Characterization of Polysaccharides Extracted from a Cultivated Brown Alga Costaria costata During the Harvest Period, Journal of Ocean University of China. 17 (2018) 1209–1217. https://doi.org/10.1007/s11802-018-3621-8.

[20] F. Shang, R. Mou, Z. Zhang, N. Gao, L. Lin, Z. Li, M. Wu, J. Zhao, Structural analysis and anticoagulant activities of three highly regular fucan sulfates as novel intrinsic factor Xase inhibitors, Carbohydrate Polymers. 195 (2018) 257–266. https://doi.org/https://doi.org/10.1016/j.carbpol.2018.04.117.

[21] C. Oliveira, S. Granja, N.M. Neves, R.L. Reis, F. Baltazar, T.H. Silva, A. Martins, Fucoidan from Fucus vesiculosus inhibits new blood vessel formation and breast tumor growth in vivo, Carbohydrate Polymers. 223 (2019) 115034. https://doi.org/https://doi.org/10.1016/j.carbpol.2019.115034.

[22] A.I. Usov, G.P. Smirnova, N.G. Klochkova, Polysaccharides of Algae: 55. Polysaccharide Composition of Several Brown Algae from Kamchatka, Russian Journal of Bioorganic Chemistry. 27 (2001) 395–399. https://doi.org/10.1023/A:1012992820204.

[23] T. Hahn, M. Schulz, R. Stadtmüller, A. Zayed, K. Muffler, S. Lang, R. Ulber, Cationic Dye for the Specific Determination of Sulfated Polysaccharides., Analytical Letters. 49 (2016) 1948–1962. http://10.0.4.56/00032719.2015.1126839.

[24] A.J. Lorbeer, S. Charoensiddhi, J. Lahnstein, C. Lars, C.M.M. Franco, V. Bulone, W. Zhang, Sequential extraction and characterization of fucoidans and alginates from Ecklonia radiata, Macrocystis pyrifera, Durvillaea potatorum, and Seirococcus axillaris, Journal of Applied Phycology. 29 (2017) 1515–1526. https://doi.org/10.1007/s10811-016-0990-5.

[25] G. Espinosa-Velázquez, A.M. Ramos-de-la-Peña, J. Montanez, J.C. Contreras-Esquivel, Rapid physicochemical characterization of innovative fucoidan/fructan powders by ATR–FTIR, Food Science and Biotechnology. 27 (2018) 411–415. https://doi.org/10.1007/s10068-017-0265-1.

[26] A. Pielesz, W. Biniaś, J. Paluch, Mild acid hydrolysis of fucoidan: characterization by electrophoresis and FT-Raman spectroscopy, Carbohydrate Research. 346 (2011) 1937–1944. https://doi.org/https://doi.org/10.1016/j.carres.2011.05.016.

[27] M. Auer, U. Griesser, J. Sawatzki, Qualitative and quantitative study of polymorphic forms in drug formulations by near infrared FT-Raman spectroscopy, Journal of Molecular Structure. 661–662 (2003) 307–317. ttps://doi.org/10.1016/j.molstruc.2003.09.002.

[28] E. Simone, A.N. Saleemi, Z.K. Nagy, Application of quantitative Raman spectroscopy for the monitoring of polymorphic transformation in crystallization processes using a good calibration practice procedure, Chemical Engineering Research and Design. 92 (2014) 594–611. https://doi.org/https://doi.org/10.1016/j.cherd.2013.11.004.

[29] E.C.Y. Li-Chan, The applications of Raman spectroscopy in food science, Trends in Food Science & Technology. 7 (1996) 361–370. https://doi.org/https://doi.org/10.1016/S0924-2244(96)10037-6.

[30] T.N. Tran, N.L. Afanador, L.M.C. Buydens, L. Blanchet, Interpretation of variable importance in Partial Least Squares with Significance Multivariate Correlation (sMC), Chemometrics and Intelligent Laboratory Systems. 138 (2014) 153–160. https://doi.org/https://doi.org/10.1016/j.chemolab.2014.08.005.

[31] M. Farrés, S. Platikanov, S. Tsakovski, R. Tauler, Comparison of the variable importance in projection (VIP) and of the selectivity ratio (SR) methods for variable selection and interpretation, Journal of Chemometrics. 29 (2015) 528–536. https://doi.org/10.1002/cem.2736.

[32] F. Allegrini, A.C. Olivieri, IUPAC-Consistent Approach to the Limit of Detection in Partial Least-Squares Calibration, Analytical Chemistry. 86 (2014) 7858–7866. https://doi.org/10.1021/ac501786u.

[33] Z. DISCHE, L.B. SHETTLES, A specific color reaction of methylpentoses and a spectrophotometric micromethod for their determination., The Journal of Biological Chemistry. 175 (1948) 595–603.
[34] A. V Skriptsova, Seasonal variations in the fucoidan content of brown algae from Peter the Great Bay, Sea of Japan, Russian Journal of Marine Biology. 42 (2016) 351–356. https://doi.org/10.1134/S1063074016040106.

[35] B. Matsuhiro, Vibrational spectroscopy of seaweed galactans, Hydrobiologia. 326 (1996) 481–489. https://doi.org/10.1007/BF00047849.

[36] B. Matsuhiro, I.O. Osorio-Román, R. Torres, Vibrational spectroscopy characterization and anticoagulant activity of a sulfated polysaccharide from sea cucumber Athyonidium chilensis, Carbohydrate Polymers. 88 (2012) 959–965. https://doi.org/https://doi.org/10.1016/j.carbpol.2012.01.052.

[37] T. Mehmood, K.H. Liland, L. Snipen, S. Sæbø, A review of variable selection methods in Partial Least Squares Regression, Chemometrics and Intelligent Laboratory Systems. 118 (2012) 62–69. https://doi.org/https://doi.org/10.1016/j.chemolab.2012.07.010.

[38] G. Cardenas-Jiron, D. Leal, B. Matsuhiro, I.O. Osorio-Roman, Vibrational spectroscopy and density functional theory calculations of poly-D-mannuronate and heteropolymeric fractions from sodium alginate, Journal of Raman Spectroscopy. 42 (2011) 870–878. https://doi.org/10.1002/jrs.2760.

[39] F. Cabassi, B. Casu, A.S. Perlin, Infrared absorption and raman scattering of sulfate groups of heparin and related glycosaminoglycans in aqueous solution, Carbohydrate Research. 63 (1978) 1–11. https://doi.org/https://doi.org/10.1016/S0008-6215(00)80924-6.

[40] R. Hilfiker, J. Berghausen, F. Blatter, A. Burkhard, S.M. De Paul, B. Freiermuth, A. Geoffroy, U. Hofmeier, C. Marcolli, B. Siebenhaar, M. Szelagiewicz, A. Vit, M. von Raumer, Polymorphism - integrated approach from high-throughput screening to crystallization optimization, Journal of Thermal Analysis and Calorimetry. 73 (2003) 429–440. https://doi.org/10.1023/A:1025409608944.

[41] M. Garcia-Vaquero, V. Ummat, B. Tiwari, G. Rajauria, Exploring Ultrasound, Microwave and Ultrasound-Microwave Assisted Extraction Technologies to Increase the Extraction of Bioactive Compounds and Antioxidants from Brown Macroalgae., Marine Drugs. 18 (2020). https://doi.org/10.3390/md18030172.

[42] H.S. Soedjak, Colorimetric Determination of Carrageenans and Other Anionic Hydrocolloids with Methylene Blue, Analytical Chemistry. 66 (1994) 4514–4518. https://doi.org/10.1021/ac00096a018.

[43] D. Ziółkowska, A. Kaniewska, J. Lamkiewicz, A. Shyichuk, Determination of carrageenan by means of photometric titration with Methylene Blue and Toluidine Blue dyes, Carbohydrate Polymers. 165 (2017) 1—6. https://doi.org/10.1016/j.carbpol.2017.02.029.

[44] L. D'Ilario, I. Francolini, A. Martinelli, A. Piozzi, Insight into the Heparin–Toluidine Blue (C.I. Basic Blue 17) interaction, Dyes and Pigments. 80 (2009) 343–348. https://doi.org/10.1016/j.dyepig.2008.07.015.

[45] Garcia-Vaquero, M. Chapter 6 - Analytical Methods and Advances to Evaluate Dietary Fiber. In Dietary Fiber: Properties, Recovery, and Applications; Galanakis, C. M., Ed.; Academic Press, 2019; pp 165-197. [46] Sigma-Aldrich. SUPELCO, Bulletin 887B. HPLC Carbohydrate ColumnSelection Guide, 1999; pp 1-8.